Experimental Investigation on Dynamic Balancing of a Turbine Rotor

N. Sai Akhil[1] A. Rithwik Reddy[2] CH. Sairam Reddy[3] G.Rahul[4] A.Suresh[5]
[1,2,3,4,5]Department of Mechanical Engineering
[1,2,3,4,5]CVR College of Engineering, Hyderabad, India

Abstract— A Turbine is a rotary engine that converts the energy from a fluid to useful work. The turbines in general carry parts as a shaft, moving Blades, a stationary (Guide) blades and a casing. Balancing is the most important operation to be carried out for any rotating element (rotor) for its smooth function and long reliable functioning. Any cause of unbalance would cause vibration and stresses in the rotor itself and to its supporting structure. The unbalance may cause the other parts of the machine to vibrate and also other adjacent machines may vibrate in resonance to this vibration, hence causing an insecure and disturbing working environment. Balancing of the rotor is, therefore, necessary to increase the quality of product, minimize the vibrations, noises, operator annoyance and fatigue, structural stresses and mainly to increase the bearing life and to minimize the power losses. The paper involves the dynamic balancing of the RINL rotor, where in vector diagrams have been drawn to calculate the amount of balancing mass to be added. The graphical and bar chart of each unbalance run have been plotted and analyzed.

Keywords: Dynamic Balancing, Turbine Rotor, RINL Turbine

I. INTRODUCTION

Generation of power in abundance is needed for any country to develop into an industrial nation [1]. It is possible to generate power using thermal, tidal or nuclear energy. Thermal power plants play a key role in the generation of power in view of the abundant coal supplies in our country. Steam turbine, mechanical rotating equipment which consists of stationary and moving blade rows, is the main component of a thermal power plant. A steam turbine based power plant involves raising high-pressure steam in a boiler from the thermal energy and expanding the steam in a turbine to generate shaft power, which in turn is converted into electricity in a generator [2].

The motive power in a steam turbine is obtained by the rate of change in momentum of a high velocity jet of steam impinging on a curved blade which is free to rotate. The steam from the boiler is expanded in a nozzle, resulting in the emission of a high velocity jet. This jet of steam impinges on the moving vanes or blades, mounted on a shaft. Here it undergoes a change of direction of motion which gives rise to a change in momentum and therefore a force [3].

The first patent for balancing was filed by Henry Martinson of Canada in 1870. Near the turn of century Akimoff (USA) and Stodola (Switzerland) attempted to develop Martinson's technology and apply it for industrial use. However, it was in 1907 when a modified version of the technology was patented by Dr. Franz Lawaczek, and offered to Carl Scheck, Darmstadt, Germany, for development [4]. Schenck built the first industrial two-plane balancer, and subsequently bought exclusive world rights to the dynamic balancing machine in 1915 [5]

II. METHODOLOGY:

A. *Analysis:*

1) *Low Speed Balancing:*

The amount to be balanced is calculated by drawing a vector diagram, the resultant thus obtained is the amount to be balanced. For the vector plot of run-0 and run-1, the resultant obtained is 288 gms (from vector sheet-1 of low speed balancing), and hence 6screws of each 53gms is added [6]. Similar additions are done for plots 1, 2 and 2, 3. The balancing is done till the resultant weight is less than 10 gms [7].

S.NO	Speed (RPM)	Sensitivity	Measured Value				Bearing. Force (Newton)		Unbalance Condition	
			Rear End (P_1)		Front End (P_2)				(Rear End)	(Front End)
			(Div)	(<Angle)	(Div)	(<Angle)	Rear End (P_1)	Front End (P_2)		
0	400	1 (gr)	1800	66^0	245	62^0				
									+6s/250 (53 gr each)	
1	400	1 (gr)	1520	67^0	105	68^0				
									+17w/250 (each 86 gr)	
2	400	1 (gr)	91	185^0	70.7	65^0				
									-1w +1w	
3	400	1 (gr)	49	274^0	26.8	228^0				

Table 1: Low Speed Balancing

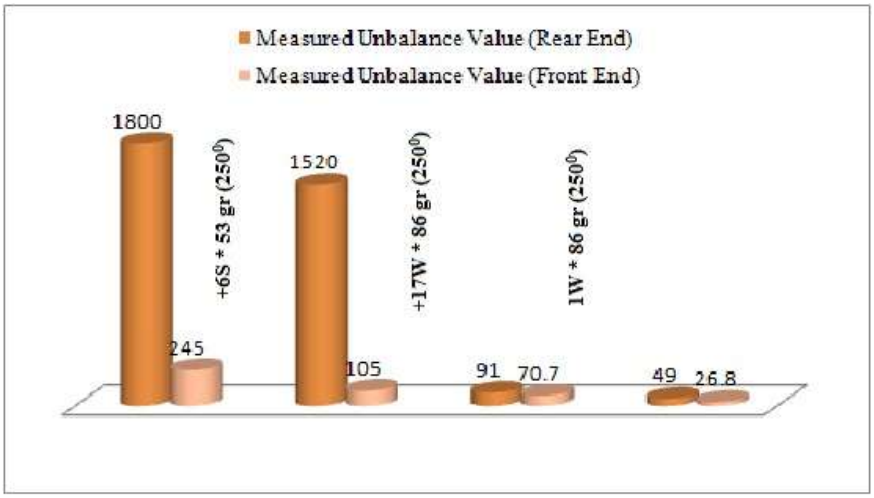

Fig. 1: Plot showing reduction in unbalance in low speed balancing

The above plotted graph is drawn between 'run number' and 'measured unbalance value' in grams, it can be inferred that, in low speed balancing (static balancing) the rotor is rotated at 400 rpm for 4 runs and the unbalance at rear and front end is measured [8].

At first run, unbalance at rear end is 1800 gms and at front end are 245 gms. This unbalance is balanced by adding 6 screws each of 53 gms at 250^0 to the rotor axis. At second run the unbalance is reduced to 1520 and 105 at rear and front ends respectively. This is balanced by adding 17 weights each of weight 86 gms at 250^0 [9].

This unbalance is further reduced in third run by 91 gms at rear and 70.7 gms at front end. In the fourth run, it is further reduced to 49 and 26.8 in the fourth run [10].

The vector plot is plotted for the above table and it is drawn for run-1 and run-2, the amount of vibration is the resultant and the amount of weight is added at an angle 180^0 to the angle of highest amplitude in the former run, i.e., at 19^0 (highest amplitude is 7.0 µm at 161^0 at front end in the above case) and hence 2 weights each 86gms is added in the front end at 10^0) 19^0 rounded to 10^0. After this the rotor is again run and the next balancing done until the bearing force for two consecutive runs reduces [11].

S.NO	Speed (RPM)	Sensitivity	Measured Value				Bearing. Force (Newton)		Unbalance Condition	
			Rear End (P_1)		Front End (P_2)				(Rear End)	(Front End)
			(Div)	(<Angle)	(Div)	(<Angle)	Rear End (P_1)	Front End P_2		
1	2000	1 (µm)	3.30	9^0	0.84	302^0				
2	2400	1 (µm)	3.61	12^0	2.83	185^0				
3	2600	1 (µm)	4.28	8^0	4.24	176^0				
4	2800	1 (µm)	5.44	355^0	5.73	167^0			176 lpm/40.9⁰	151 lpm/57⁰
5	3000	1 (µm)	6.43	342^0	7.0	161^0	4319	4875		+2w/10⁰ (each 86g)

Table 2: Balancing of Steam Turbine, Run No: 1

2) Balancing Process-1 (Run-1):

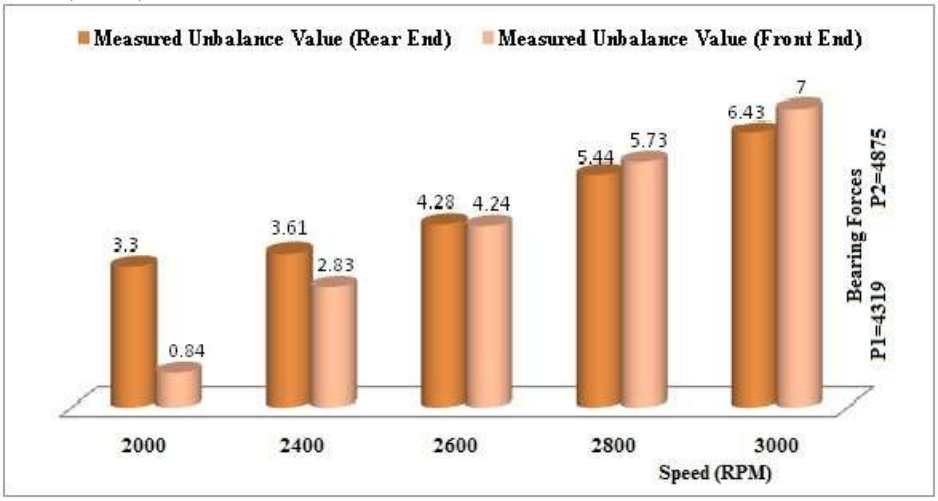

Fig. 2: Plot showing variation of amplitude with speed

This graph is drawn for dynamic balancing. The rotor is rotated from 2000 – 3000 rpm (operating speed) and unbalance is found at rear and front ends. A graph is drawn between speed and measured unbalance. The bearing forces at rear and front ends after run-1 are 4319N and 4875N; these forces are to be minimized [12].

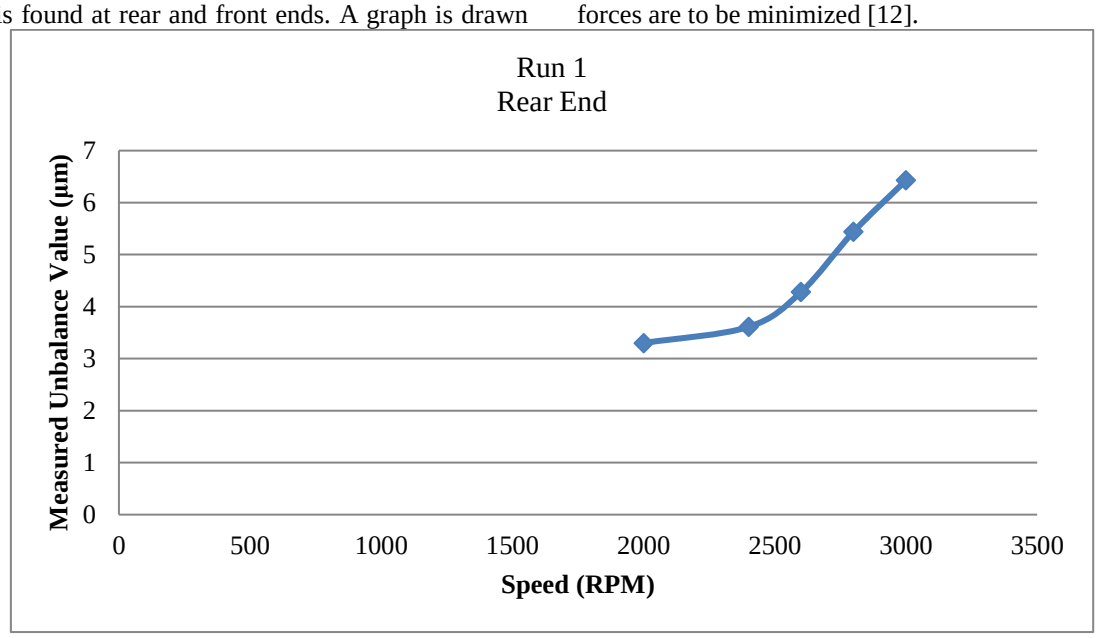

Fig. 3: Speed Vs Measured Unbalance Value Plot at Rear End for Run-1

This is the graph showing the unbalance value at run1 at different speeds from 2000 rpm to 3000 rpm (operating speed) , at rear end. The unbalance is high at operating speed, it is to be reduced.

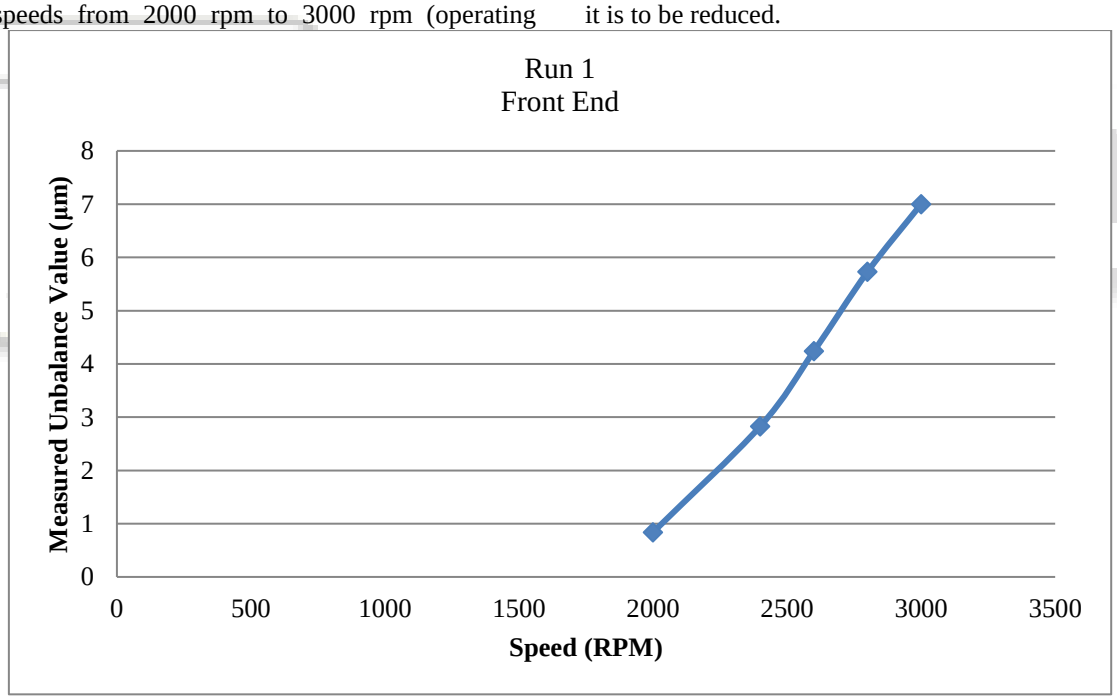

Fig. 4: Speed Vs Measured Unbalance Value Plot at Front End for Run-1

A Similar plot in the front end shows an increase in the amplitude of vibrations, as the bearing forces vary in proportional to the amplitude of vibration, the bearing forces are high with higher amplitudes. Hence, the bearing forces thus the amplitude of vibration should be brought down to a reasonable value by adding balance masses [13,14].

Results and Discussion:

The low speed balancing has been commenced for four runs and the speed value is decided as less than $1/3^{rd}$ of the operating speed. The initial run (run-0) gives an unbalance and for run-1 also there is an unbalance, a vector plot drawn shows the resultant of unbalance and the amount to be balanced. Consider the vector plot of low speed balancing for run-0 and run-1, the resultant C_0C_1 =288gms and F_0F_1=180gms, therefore the amount of unbalance is more at the couple end (rear end) and hence the weights are added at the rear end in opposite to the angle of the unbalance, i.e., in low speed balancing table it is seen that 1800gms unbalance is at rear end at 66^0 and 245gms at the front end at 62^0, therefore the weights are added at an angle of $66^0 + 180^0$ i.e., opposite to the higher unbalance value, and hence the amount to be added is 288gms at 246^0 and the amount added is 6 screws each of 53gms (=318gms) at 250^0.

The above procedure is repeated until an unbalance value of less than 50gms is achieved and this is achieved after the fourth run which is shown in plot no.1 and hence achieved.

The next step is the high speed balancing where in the focus is on the bearing forces mainly at the critical speed and hence at the operating speed. The vector plot should be hence drawn at both the critical and operating speeds. Consider an example of the run -2 and run-3 of the rotor. The amplitude of vibrations is recorded and the vector diagrams are drawn taking to a suitable scale. The resultant of the vector is calculated and the bearing force for that resultant is calculated. The trial mass is added based on the amplitude of vibration i.e., more the unbalance more is the mass added. The position of the mass to be added is proportional to the position of unbalance. In the table 4.3 it can be seen that the amplitudes at the operating speeds at the rear and front end are 7.34µm and 8.3µm, at 119^0 and 272^0 respectively. Hence, the balance is to be done for the amplitude of 8.3µm, i.e., at the front end at an angle of 40^0.

The resultant vibration amplitude is measured and the bearing forces at this resultant are calculated. The same procedure is followed for all the runs at operating speeds and also at the critical speeds. The same is done until two resultant values of the resultant bearing forces get decreased. This aspect is noticed in the vector plots between the runs, run-3 and run-4 and between run-4 and run-5, where in there is a decrease in the bearing force values and hence the rotor needs no additional balance after run-5.

After this run, the rotor is run for its final balance where the bearing forces at all the speeds is written down in the balance sheet and the rotor is withdrawn from the setup.

The sheet (table 4.7) shows the values of the bearing forces at all speeds after the rotor balancing has been done and hence it can noticed that the values of the bearing forces are well within the limits.

The permissible limits for bearing forces for the rotor are:

Parameter	Rear End(N)	Front End(N)
Operating Speed (3000 RPM)	9,510N	8,251N
Critical Speed (1567 RPM)	13,586N	11,788N

The obtained values are:

Parameter	Rear End(N)	Front End(N)
Operating Speed (3000 RPM)	1,792N	2,739N
Critical Speed (1567 RPM)	3,157N	2,863N

III. CONCLUSION:

The experiment is mainly done to bring down the bearing forces at the critical and operating speeds to avoid the damage of bearings and the rotor to promote long run and to increase the life of the turbine. The bearing forces are calculated as a product of the pedestal stiffness constant and amplitude of vibration at that speed, both changing as speed changes.

After the initial balance, i.e., low speed balance, where the rotor is balanced at 1/3 of the operating speed, the rotor is run with increasing speed to notice the critical speed where the sudden change in amplitude is noticed. The trial mass is continuously added until the bearing force at critical speed shows two consecutive drops and then the final balance sheet is prepared where the amplitude of vibrations and bearing forces at different speeds of the rotors is shown.

Hence, two consecutive drops of bearing forces is noticed in the vector plot between run no.3, run no.4 and run no.4 and run no.5. Therefore, the bearing forces for the rotor at both the critical speed and the operating are brought within the limits which are 9510N and 8251N at rear and front end respectively at operating conditions and 13,586N and 11,788N at rear and front end for critical speed. The achieved values being1792N and 2739N for front and rear ends at operating speed; and 3157N and 2863N for rear and front end at critical speed.

REFERENCES:

[1] Deng, W.Q.; Tang, G.; Gao, D.P. Research summary of rotor dynamic characteristics and dynamic balance. Gas Turbine Exp. Res. 2018, 21, 57–62. (In Chinese)
[2] Bin, G.; Yao, J.; Jiang, Z.; Gao, J. Solving method of influence coefficient for rotor dynamic balance based on finite element model. J. Vib. Meas. Diagn. 2017, 33, 998–1002. (In Chinese)
[3] Urbikain, G.; Alvarez, A.; López de Lacalle, L.N.; Arsuaga, M.; Alonso, M.A.; Veiga, F. A Reliable Turning Process by the Early Use of a Deep Simulation Model at Several Manufacturing Stages. Machines 2017, 5, 15. [CrossRef]
[4] Huang, W.H.; Wu, X.H.; Jiao, Y.H.; Xia, S.B.; Chen, Z.B. Review of nonlinear rotor dynamics. J. Vib. Eng. 2020, 33, 5–17.
[5] Green, K.; Champneys, A.R.; Lieven, N.J. Bifurcation analysis of an automatic dynamic balancing mechanism for eccentric rotors. J. Sound Vib. 2016, 391, 861–881
[6] Zheng, L.X.; Gao, X.G.; Li, X.F. Transient field balancing technique for a micro turbo-jet engine. Meas. Diagn. 2018, 28, 282–285.
[7] Fu, C.; Ren, X.M.; Yang, Y.F.; Deng, W.Q. Transient dynamic balancing of rotor system with parameter uncertainties. J. Dyn. Control 2017, 15, 453–458.
[8] Huang, X.; Zhou, J.P.; Wen, G.R.; Jiang, H.; Tan, Y. Balancing under all working conditions of rotor based on parameterized time-frequency analysis. J. Vib. Meas. Diagn. 2017, 37, 134–139.
[9] Han, J.; Gao, D.P.; Hu, X.; Chen, G. Research on beat vibration of dual-rotor for aero-engine. Acta Aeronaut. Et Astronaut. Sin. 2017, 28, 1369–1373.
[10] Deepthikumar, M.B.; Sekhar, A.S.; Srikanthan, M.R. Modal balancing of flexible rotors with bow and distributed unbalance. J. Sound Vib. 2019, 338, 6216–6233.
[11] Liu, G.Q.; Zheng, L.X.; Mei, Q.; Huang, J.J. Balancing method of flexible rotor across second order without trial weights. Acta Aeronaut. Et Astronaut. Sin. 2018, 35, 1019–1025
[12] Chen, X.; Liao, M.F.; Zhang, X.M.; Wang, S.J. Field balancing technology for low pressure rotors of high bypass ratio turbofan engines. Hangkong Dongli Xuebao/J. Aerosp. Power 2019, 35, 808–819.

[13] Tresser, S.; Dolev, A.; Bucher, I. Dynamic balancing of super-critical rotating structures using slow-speed data via parametric excitation. J. Sound Vib. 2018, 415, 59–77.
[14] Saldarriaga, M.V.; Steffen, V.; Der Hagopian, J.; Mahfoud, J. On the balancing of flexible rotating machines by using an inverse problem approach. J. Vib. Control 2021, 17, 1021–1033.

